First published in:

Available online at www.sciencedirect.com

ScienceDirect

Comput. Methods Appl. Mech. Engrg. 197 (2008) 3045–3056

Computer methods in applied mechanics and engineering

www.elsevier.com/locate/cma

On the solvability of closest point projection procedures in contact analysis: Analysis and solution strategy for surfaces of arbitrary geometry

Alexander Konyukhov, Karl Schweizerhof *

University of Karlsruhe, Institute of Mechanics, Kaiserstrasse 12, D-76128 Karlsruhe, Germany

Received 19 March 2007; received in revised form 5 October 2007; accepted 8 February 2008
Available online 10 March 2008

Abstract

The uniqueness and existence of the closest point projection procedure widely used in contact mechanics are analyzed in the current article. First, a projection domain for C^2-continuous surfaces is created based on the geometrical properties of surfaces. Then any point from the projection domain has a unique projection onto the given surface. It is shown that in order to construct a continuous projection domain for arbitrary globally C^1, or C^0-continuous surfaces, a projection routine should be generalized and also include a projection onto a curved edge and onto corner points. Criteria of uniqueness and existence of the corresponding projection routine are given and discussed from the geometrical point of view. Some examples showing the construction of the projection domain as well as the necessity of a generalized projection routine are given.

Keywords: Closest point projection; Uniqueness and existence; Contact; Covariant description

1. Introduction

The so-called closest point projection procedure is often introduced as a numerical scheme to compute coordinates of a point projected onto a surface. In variational formulations for contact problems it appears due to the split of contact displacements into a normal and a tangential part. In early publications for finite element models it was explained as a result of the linearization of non-penetration conditions [12]. Hallquist et al. [5] considered the split into normal and tangential direction via the projection operation for a so-called "master–slave" approach within the finite element contact model. Such an approach is based on looking at normal contact where a "slave" node of one body penetrates into a "master" segment of another body. The value of penetration is measured as the closest distance to the master body. In a next step of the contact algorithm, the penalty method together with explicit time integration was used to enforce the contact conditions. For an implicit solution Wriggers and Simo [28] proposed a consistent linearization procedure of the penalty functional containing the penetration function and obtained the corresponding tangent stiffness matrices within the Newton iteration scheme. However, the penetration function based on the closest point projection is not only used for formulations in combination with a penalty functional, but also in other computational schemes to enforce the condition of non-penetration in contact. The concept of the closest distance is also important for contact searching routines in order to define potentially contacting points.

In order to show the importance of the projection operation, we briefly focus here on methods in contact mechanics, where the closest point procedure occurs. Contact

* Corresponding author. Tel.: +49 721 608 3715; fax: +49 721 608 7990.
E-mail addresses: Alexander.Konyukhov@ifm.uni-karlsruhe.de (A. Konyukhov), Karl.Schweizerhof@ifm.uni-karlsruhe.de (K. Schweizerhof).
URLs: http://www.ifm.uni-karlsruhe.de/seite_203.php (A. Konyukhov), http://www.ifm.uni-karlsruhe.de (K. Schweizerhof).

0045-7825/$ - see front matter © 2008 Elsevier B.V. All rights reserved.
doi:10.1016/j.cma.2008.02.009

elements for bilinear surface approximations based on the penalty method for non-frictional problems are discussed in Parisch [21]. Due to decoupling of normal and tangential forces the projection procedure necessarily appears for 2D frictional problems in Giannakopoulos [4] and Wriggers et al. [29], then also for 3D problems in Peric and Owen [23] and in Parisch and Lübbing [22]. All mentioned references combine the penalty method together with the regularization of the Coulomb friction model and a radial-return algorithm within the friction algorithm. This algorithm is predominantly used in computational plasticity, see Simo and Hughes [27], and also exploits the closest point procedure; however, then the projection is given onto the yield surface in the force space. Full Lagrange multipliers methods are standard for enforcing constraints in computational mechanics, but cannot be easily transported into frictional problems using the same penetration, or distance function as mentioned above, see the review in Zhong [31]. This is due to the nature of friction forces depending on velocity and, therefore, requiring an incremental update procedure. For a small sliding problem, a perturbed Lagrangian method including both penalty and Lagrangian functionals was discussed in Wriggers and Simo [28]. Then augmented Lagrangian methods appeared to be more robust. Thus, a 2D finite element algorithm based on the augmented Lagrangian method has been proposed in Wriggers et al. [29]. A mixed penalty–duality approach based on the augmented Lagrangian scheme is proposed in Alart and Curnier [2], where different distance functions have been discussed. Laursen and Simo [20] formulated contact conditions via convective coordinates on the contact surface within both, the penalty method and the augmented Lagrangian method. For various geometrical situations the method has been discussed in Heegaard and Curnier [6] for large-slip problems, in Heege and Alart [8] for contact with CAD surfaces and in Pietrzak and Curnier [24] for finite deformations and large sliding. The full Lagrangian approach for frictional problems has been discussed in Jones and Papadopoulos [11] utilizing stick-to-slide conditions in one step, and therefore, covering only small sliding problems. More recently the so-called mortar method, originally based on Lagrangian multipliers enforcing the non-penetration conditions is considered in Hüeber and Wohlmuth [9] for non-frictional problems, where a special discretization technique has been taken for the Lagrange multiplier functions. A mortar scheme based on a special integration technique for constraint equations is proposed in Puso and Laursen [25] for non-frictional problems and extended into the frictional case via the augmented Lagrangian method by the same authors [26].

The publications listed above cover the most applied methods in computational contact mechanics and all contain the closest point procedure as the first necessary step. Despite the enormous number of publications on contact mechanics, there are only a few publications covering to some completeness the problem of uniqueness and existence of the closest point procedure for arbitrary approximations of the contact surfaces as well as describing effective numerical algorithms to overcome problems. The problem of non-uniqueness and non-existence of the projection for, e.g. bilinear approximations of a surface by finite elements is known since the first publications, see Hallquist et al. [5], and mostly reported in theoretical manuals of popular commercial codes, see [10,1]. Heegaard and Curnier in [7] mentioned that geometrical parameters of a surface, such as a focal point can be used to determine existence and uniqueness of the projection for smooth surfaces. However, for arbitrary surfaces described, e.g. by CAD-systems and containing combinations of smooth surfaces, curved edges and corner points, the situation can be far more complex. Some techniques dealing with non-existence of the projection in certain cases are well known, e.g. a situation when the slave point is passing over the edge of a locally concave part of a body can be overcome by taking an average vector from the normals of neighboring contact surface segments. A description of this rather heuristic approach can be found in the books of Wriggers [30] and Laursen [19] as well as in theory manuals [10,1]. This technique is used in a similar manner in multi-surface plasticity when the C^1-continuity of the yield surface is broken, see Simo and Hughes [27]. Other techniques such as the projection onto the edge for such cases, see e.g. in Heegaard and Curnier [6] and in Zhong and Nilsson [32], are also reported to be implemented in commercial programs [10].

In the current contribution, we provide analytical tools allowing to create, a priori, *proximity domains of contact surfaces* from which a given contact point is always uniquely projected. This approach is based on the geometrical properties of contact surfaces exploiting the covariant description for contact problems developed in Konyukhov and Schweizerhof [13,14]. First, all C^2-continuous surfaces are classified according to their differential properties allowing a unique projection. Then, *proximity domains* are created for C^1-continuous surfaces. Finally, *proximity domains* are proposed for globally C^0-continuous surfaces covering all practical approximations. The projection scheme in the latter case is further generalized including the projection onto geometrical objects of lower order (curved edges, corner points). In such cases the corresponding proximity domains are created by a geometrical analysis of those objects. Also the reduction into the 2D plane case is discussed. The examples are chosen to show the necessity of the proposed generalized projection procedure in certain mechanical problems as well as the necessity of the proximity domain for searching techniques when a contact surface is given by arbitrary discretization, e.g. described by CAD-systems, or found in high order FEM analysis.

2. Formulation of the closest point projection procedure in geometrical terms

The most important operation for the data transfer between contacting bodies in contact mechanics is the clos-

est point projection procedure, see Fig. 1, where one seeks the projection of a given contact point from one body $\mathbf{r}$, usually called a slave point, onto another contact body, usually called a master body, parameterized as

$$\boldsymbol{\rho} = \boldsymbol{\rho}(\xi^1, \xi^2). \tag{1}$$

The parameterization (1) by Gaussian coordinates is arbitrary and ξ^1, ξ^2 can be provided either by, e.g. a finite element approximation, or by a spline approximation or by a NURBS approximation. The closest point procedure appears also in many other applications such as fluid-structure interactions, computational plasticity and others. The projection problem is formulated as an extremal problem

$$\|\mathbf{r} - \boldsymbol{\rho}(\xi^1, \xi^2)\| \to \min, \quad \to (\mathbf{r} - \boldsymbol{\rho}) \cdot (\mathbf{r} - \boldsymbol{\rho}) \to \min, \tag{2}$$

which is solved then mostly numerically. However, then a fundamental problem arises: Does the solution of (2) exist? And, if it exists, then, is it unique for any arbitrary surface approximation?

The direct and strict answer is fully covered by the application of the famous theorem from the convex analysis to problem (2), see e.g. [3].

If the function

$$\mathbf{F}(\xi^1, \xi^2) = \frac{1}{2}(\mathbf{r} - \boldsymbol{\rho}) \cdot (\mathbf{r} - \boldsymbol{\rho}) \tag{3}$$

is convex in a domain $(\xi^1, \xi^2) \in D$, then the solution of problem (2) exists and is unique in this domain.

This leads to the fact that the solution can be obtained numerically by, e.g. a Newton iteration procedure, which will converge from any initial point inside the domain $(\xi^1_{(0)}, \xi^2_{(0)}) \in D$.

Using this criterion we can focus on the geometrical properties of the surfaces. Then the goal of this contribution is to create a classification of surfaces from its differential geometry point of view onto which a point can be projected uniquely.

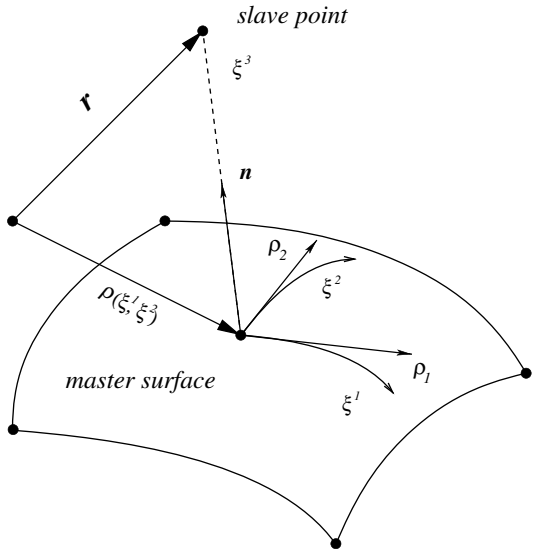

Fig. 1. Closest point procedure and definition of the spatial coordinate system.

The analysis of the local geometrical structure of surfaces allows to create *a projection domain* Ω in 3D from which any point can be uniquely projected onto the given surface. Starting with the C^2-continuous case, we will consider also cases possessing parts with solely C^1- and C^0-continuity discussing the solvability of problem (2) and in addition the possible multiplicity of solutions.

Assuming that the function $\mathbf{F}$ is twice differentiable, i.e. for C^2-continuous surfaces, we can construct the Newton iterative process for the solution of the minimization problem (2) as follows:

$$\begin{aligned} \Delta\boldsymbol{\xi}_{(n)} &= \begin{bmatrix} \Delta\xi^1_{(n)} \\ \Delta\xi^2_{(n)} \end{bmatrix} = -(\mathbf{F}'')^{-1}_{(n)}\mathbf{F}'_{(n)}, \\ \boldsymbol{\xi}_{(n+1)} &= \boldsymbol{\xi}_{(n)} + \Delta\boldsymbol{\xi}_{(n)}, \end{aligned} \tag{4}$$

where the first derivative $\mathbf{F}'$ and the second derivative $\mathbf{F}''$ with respect to the surface coordinates ξ^1, ξ^2 are computed as

$$\mathbf{F}' = \begin{bmatrix} \frac{\partial F}{\partial \xi^1} \\ \frac{\partial F}{\partial \xi^2} \end{bmatrix} = -\begin{bmatrix} \boldsymbol{\rho}_1 \cdot (\mathbf{r} - \boldsymbol{\rho}) \\ \boldsymbol{\rho}_2 \cdot (\mathbf{r} - \boldsymbol{\rho}) \end{bmatrix}, \tag{5}$$

$$\mathbf{F}'' = \begin{bmatrix} \boldsymbol{\rho}_1 \cdot \boldsymbol{\rho}_1 - \boldsymbol{\rho}_{11} \cdot (\mathbf{r} - \boldsymbol{\rho}) & \boldsymbol{\rho}_1 \cdot \boldsymbol{\rho}_2 - \boldsymbol{\rho}_{12} \cdot (\mathbf{r} - \boldsymbol{\rho}) \\ \boldsymbol{\rho}_2 \cdot \boldsymbol{\rho}_1 - \boldsymbol{\rho}_{21} \cdot (\mathbf{r} - \boldsymbol{\rho}) & \boldsymbol{\rho}_2 \cdot \boldsymbol{\rho}_2 - \boldsymbol{\rho}_{22} \cdot (\mathbf{r} - \boldsymbol{\rho}) \end{bmatrix}. \tag{6}$$

Here a short notation for the partial derivatives has been introduced as

$$\boldsymbol{\rho}_i = \frac{\partial \boldsymbol{\rho}}{\partial \xi^i}, \quad \boldsymbol{\rho}_{ij} = \frac{\partial^2 \boldsymbol{\rho}}{\partial \xi^i \partial \xi^j}. \tag{7}$$

Now, we introduce a 3D spatial coordinate system related to the surface coordinate system, see Fig. 1, as follows:

$$\mathbf{r}(\xi^1, \xi^2, \xi^3) = \boldsymbol{\rho} + \mathbf{n}\xi^3. \tag{8}$$

All necessary parameters are defined in the covariant basis of the surface tangent vectors $\boldsymbol{\rho}_1, \boldsymbol{\rho}_2$ and a unit normal vector $\mathbf{n} = \frac{\boldsymbol{\rho}_1 \times \boldsymbol{\rho}_2}{\|\boldsymbol{\rho}_1 \times \boldsymbol{\rho}_2\|}$. The solvability of the minimization problem (2) will be considered in this coordinate system. The introduction of such a coordinate system is the basis of the covariant description for contact problems, developed in Konyukhov and Schweizerhof [13,14] for isotropical frictional problems, and then in [16,17] for anisotropic frictional problems. The dominantly geometrical structure of all contact parameters is among the main advantages of this description, e.g. a value of penetration is simply the third convective coordinate ξ^3.

The following surface tensors are used to describe the metric and the curvature properties of surfaces in differential geometry [18]:

(a) metric tensor with components:

$$a_{ij} = \boldsymbol{\rho}_i \cdot \boldsymbol{\rho}_j, \tag{9}$$

(b) curvature tensor with components:

$$h_{ij} = \boldsymbol{\rho}_{ij} \cdot \mathbf{n}, \tag{10}$$

Inserting now Eq. (8) into Eq. (6) and using the notations given in Eqs. (9) and (10) we obtain the expression $\mathbf{F}''$ in the introduced spatial coordinate system as

$$\mathbf{F}'' = \begin{bmatrix} a_{11} - \xi^3 h_{11} & a_{12} - \xi^3 h_{12} \\ a_{21} - \xi^3 h_{21} & a_{22} - \xi^3 h_{22} \end{bmatrix}. \tag{11}$$

Let us start with a case assuming a unique projection: In this case the function $\mathbf{F}$ must be convex. As is known for the convexity of $\mathbf{F}$, the second derivative $\mathbf{F}''$ must then be a positive definite matrix. Thus, the Sylvester criterion from basic algebra is exploited to check the positivity of the matrix given in Eq. (11):

$$\begin{aligned} &(a_{11} - \xi^3 h_{11}) > 0, \\ &\det[(a_{ij} - \xi^3 h_{ij})] > 0. \end{aligned} \tag{12}$$

2.1. Necessary information about the surface structure

Surprisingly, the second equation in (12) is similar to that which is used in differential geometry for the analysis of the surface structure. To emphasize this, we present here main formulae necessary for the further developments. For more information including the specific derivations of the formulae, see e.g. in [18].

The geometrical analysis of the surface structure is given by the generalized eigenvalue problem:

$$(h_{ij} - k a_{ij}) e_j = 0, \tag{13}$$

which leads to the real roots k_1, k_2 of the equation

$$\det[(h_{ij} - k a_{ij})] = 0. \tag{14}$$

These roots are called *principal curvatures* and correspond to the orthogonal *principal directions* $\mathbf{e_1}$, $\mathbf{e_2}$. The principal curvature k_1 (resp. k_2) is the curvature of a line arising from the intersection of the surface with the plane containing both, normal vector $\mathbf{n}$ and principal vector $\mathbf{e_1}$ ($\mathbf{e_2}$). Their inverse values are principal radii $R_i = 1/k_i$, see Fig. 2. The local structure of the surface in the vicinity of the computed contact point can be then classified by the Gaussian curvature K

$$K = k_1 \cdot k_2 \tag{15}$$

into four cases as follows:

(1) $K = k_1 \cdot k_2 > 0$ – an elliptic point, i.e. a surface in vicinity of the point *looks like an elliptic paraboloid*, see Fig. 2.
(2) $K = k_1 \cdot k_2 < 0$ – a hyperbolic point, i.e. a surface *looks like a hyperbolic paraboloid*, see Fig. 3. For the case with zero Gaussian curvature $K = 0$ a more careful analysis is required.
(3) Either $k_1 = 0,\ k_2 \neq 0$, or $k_2 = 0,\ k_1 \neq 0$ – a parabolic point. A surface *looks then like a parabolic cylinder*, see Fig. 4. If these conditions are fulfilled for each point of the surface, then *a flat surface* is obtained. This surface (e.g. a cylinder, or a cone) can be unwrapped on a plane.
(4) Both $k_1 = 0$ and $k_2 = 0$ – a planar point. The local structure can not be identified without the analysis of the higher order derivatives. Nevertheless, the case with $k_1 = 0$, $k_2 = 0$ for each point leads to a plane in 3D.

Eq. (14) for a definition of the principal curvatures can be written in the following form:

$$k^2 - 2Hk + K = 0 \ \Rightarrow\ k_{1,2} = H \pm \sqrt{H^2 - K} \tag{16}$$

where the Gaussian curvature K is defined as

$$K = k_1 \cdot k_2 = \frac{\det[h_{ij}]}{\det[a_{ij}]} = \frac{h_{11}h_{22} - h_{12}^2}{a_{11}a_{22} - a_{12}^2} \tag{17}$$

and the mean curvature H is defined as

$$H = \frac{1}{2}(k_1 + k_2) = \frac{1}{2}\frac{a_{22}h_{11} - 2a_{12}h_{12} + a_{11}h_{22}}{a_{11}a_{22} - a_{12}^2}. \tag{18}$$

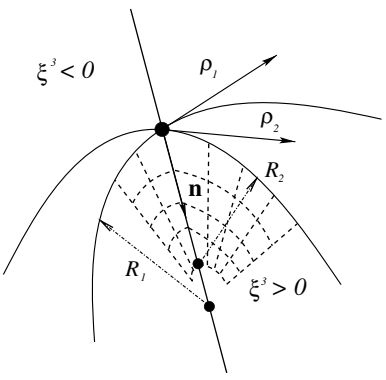

Fig. 2. Elliptic point. Structure of the surface and projection domain assuming C^2-continuity.

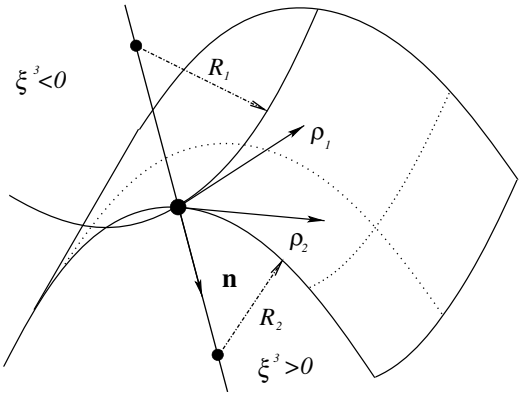

Fig. 3. Hyperbolic point. Structure of the surface and projection domain assuming C^2-continuity.

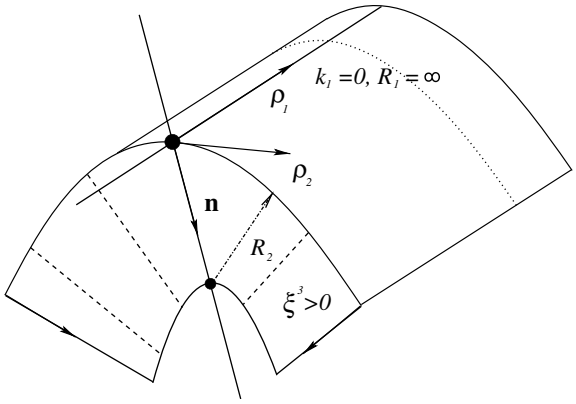

Fig. 4. Parabolic point. Structure of the surface and projection domain assuming C^2-continuity.

Remark. Any other structure of the surface in the vicinity of a point different from the described cases (1)–(3) (e.g. edge point, etc.) can arise either from a planar point (case 4), or from violation of the a priori assumed C^2-continuity and a more advanced analysis would be necessary. Surfaces with more complicated local structure leading, e.g. to a so-called "star"-looking domain, self-contacting and self-penetrating surfaces, etc. are relatively seldom in practical applications and are out of the scope of the current contribution.

3. Proximity criteria for different surfaces

In this section we consider the structure of 3D domains (*proximity domains*) surrounding a given surface, from which a point can be a priori uniquely projected onto the surface. This structure depends on the classification of surface points given in Section 2.1. Taking into account Eq. (16) for principal curvatures, the Sylvester criteria in Eq. (12) can be written in the following form:

$$\begin{aligned} &(a_{11} - \xi^3 h_{11}) > 0, \\ &\left(\frac{1}{\xi^3}\right)^2 - 2H\frac{1}{\xi^3} + K > 0. \end{aligned} \tag{19}$$

This system of inequalities can be reformulated in terms of principal curvatures k_1, k_2 as

$$\begin{aligned} &\left(\frac{1}{\xi^3} - k_1\right) > 0, \\ &\left(\frac{1}{\xi^3} - k_1\right)\left(\frac{1}{\xi^3} - k_2\right) > 0. \end{aligned} \tag{20}$$

Within the last transformation, it was assumed that the coordinate ξ^3 is a positive value into the normal vector direction $\mathbf{n}$, as chosen in Eq. (8). Thus, zones with positive and negative coordinates ξ^3 should be distinguished.

3.1. Projection domains for an elliptic point

According to the geometry presented in Fig. 2, a normal $\mathbf{n}$ is pointing into a convex part, where $\xi^3 > 0$ and, both $k_1 > 0$ and $k_2 > 0$.

3.1.1. Domain for the convex part $\xi^3 > 0$

Using the geometrical interpretation of the principal curvatures as principal radii $R_i = 1/k_i$, Eq. (20) can be written as

$$\begin{aligned} &R_1 - \xi^3 > 0, \\ &(R_1 - \xi^3)(R_2 - \xi^3) > 0. \end{aligned} \tag{21}$$

The solution allows to create a projection domain $\Omega(\xi^1, \xi^2, \xi^3)$ with a parameter $\hat{\xi}^3 = \min\{R_1, R_2\}$ with an a priori unique solution of the projection problem, see Fig. 2:

$$\Omega(\xi^1, \xi^2, \xi^3) := \{\mathbf{r} = \boldsymbol{\rho} + \xi^3\mathbf{n}, \text{ where } 0 < \xi^3 < \hat{\xi}^3\}. \tag{22}$$

This domain is created in the local coordinate system and contains all points between the original surface and shifted by $\mathbf{n}\xi^3$ surface.

3.1.2. Domain for the concave part $\xi^3 < 0$

In this case, criterion (21) is automatically fulfilled leading to an infinite domain Ω above the surface:

$$\Omega(\xi^1, \xi^2, \xi^3) := \{\mathbf{r} = \boldsymbol{\rho} + \xi^3\mathbf{n} \text{ with } -\infty < \xi^3 < 0\}. \tag{23}$$

3.2. Projection domain for a hyperbolic point

Considering a situation as presented in Fig. 3, in the case with $\xi^3 > 0$, where a projection domain is created as an overlapping of the semi-infinite domain due to the line with negative curvature k_1 and the finite domain due to the line with positive curvature k_2 similar to the domain as for a convex part for an elliptic point. The case with $\xi^3 < 0$ leads to a projection domain constructed in an identical fashion. Summarizing both cases, a finite projection domain $\Omega(\xi^1, \xi^2, \xi^3)$ is created as a domain between two shifted surfaces:

$$\Omega(\xi^1, \xi^2, \xi^3) := \{\mathbf{r} = \boldsymbol{\rho} + \xi^3\mathbf{n}, \text{ where } -R_1 < \xi^3 < R_2\}. \tag{24}$$

3.3. Projection domain for a parabolic point

A projection domain for a parabolic point, see Fig. 4, consists of a finite domain for the convex part with $\xi^3 > 0$, and a semi-infinite domain for the concave part with $\xi^3 < 0$. Thus, the projection domain $\Omega(\xi^1, \xi^2, \xi^3)$ is described as follows:

$$\Omega(\xi^1, \xi^2, \xi^3) := \{\mathbf{r} = \boldsymbol{\rho} + \xi^3\mathbf{n}, \text{ where } -\infty < \xi^3 < R_2\}. \tag{25}$$

3.4. Discussion about planar points – required approximation for the plane

As mentioned in Section 2.1 case (4), the structure of a surface in the vicinity of the planar point requires an analysis of the higher order derivatives with respect to the sur-

face coordinates. In this case, it is also difficult to discuss the convergence of the Newton iterative process (4). However, for the plane with zero curvature tensor $h_{ij} = 0$ criterion (12) becomes

$$\det[a_{ij}] > 0. \tag{26}$$

Since the metric tensor a_{ij} is always positive, a trivial result is recovered: The projection onto a plane always exists and is unique. Nevertheless, from the numerical point of view it is necessary to avoid cases with $\det[a_{ij}] \approx 0$. In such cases the angle between the convective coordinate lines is close either to 0° or to 180°, which is normally avoided *ab initio* as, e.g. in finite element approximations this would be a sign for inadmissibly distorted elements.

4. Solvability of the projection algorithm – allowable and non-allowable domains

In the previous section, the projection domains were constructed under the main assumption of sufficient smoothness of the corresponding surfaces, specifically C^2-continuity was necessary to derive all curvature parameters. In this section, we will obtain that C^1-continuity of a surface is sufficient for the construction of a continuous projection domain, while violation of C^1-continuity can cause either multiplicity of solutions, or non-existence of solutions at all. Starting with a 2D case as a preliminary case, we then develop "a remedy" for globally C^0-continuous surfaces by constructing a continuous projection domain allowing unique projections onto the surface. A generalized projection procedure includes then several projection procedures onto curved edges and corners.

4.1. Reduction to 2D plane geometry – solvability criteria and uniqueness

A covariant approach for contact problems allows to look at a 2D case either as a special reduction from a cylindrical geometry in 2D space, or as a case based on a 2D plane curve geometry, see [15]. In the last case, the length of a curved line s is used as a convective coordinate. The closest point projection method (2) is then formulated as follows:

$$F = \frac{1}{2}\|\mathbf{r} - \boldsymbol{\rho}(s)\|^2 \to \min. \tag{27}$$

A curvilinear coordinate system in 2D is based on a flat curve geometry and is introduced as follows:

$$\mathbf{r}(s,\zeta) = \boldsymbol{\rho}(s) + \zeta\boldsymbol{\nu}. \tag{28}$$

A second derivative with respect to s in this coordinate system is computed as

$$\begin{aligned} F'' &= \frac{\partial\boldsymbol{\rho}}{\partial s}\cdot\frac{\partial\boldsymbol{\rho}}{\partial s} - \frac{\partial^2\boldsymbol{\rho}}{\partial s^2}\cdot(\mathbf{r} - \boldsymbol{\rho}(s)) \\ &= \boldsymbol{\tau}\cdot\boldsymbol{\tau} - \frac{\partial\boldsymbol{\tau}}{\partial s}\cdot(\mathbf{r} - \boldsymbol{\rho}(s)). \end{aligned} \tag{29}$$

For further transformation it is necessary to introduce the Serret–Frenet formulae

$$\boldsymbol{\tau} = \frac{\partial\boldsymbol{\rho}}{\partial s}, \quad \frac{\partial\boldsymbol{\tau}}{\partial s} = k\boldsymbol{\nu}, \tag{30}$$

where $\boldsymbol{\tau}$ is a unit tangent vector, $\boldsymbol{\nu}$ is a unit normal vector and k is a curvature of the curve (the radius of the curvature $R = \frac{1}{k}$ is also often used). Taking into account the Serret–Frenet formulae together with Eq. (28) the second derivative F'' is transformed as

$$F'' = 1 - k\zeta. \tag{31}$$

Since the normal vector $\boldsymbol{\nu}$ is always pointing to the center of curvature C_1, see Fig. 5, we obtain from the condition $F'' = 1 - k\zeta > 0$ a finite projection domain $O_1O_2C_2C_1$ for the convex part as follows:

$$\Omega(s,\zeta) := \{\mathbf{r} = \boldsymbol{\rho}(s) + \zeta\boldsymbol{\nu} \text{ with } 0 < \zeta < \frac{1}{k} = R\}, \tag{32}$$

and a semi-infinite projection domain for the concave part above the curve O_1O_2:

$$\Omega(s,\zeta) := \{\mathbf{r} = \boldsymbol{\rho}(s) + \zeta\boldsymbol{\nu} \text{ with } -\infty < \zeta < 0\}. \tag{33}$$

The case with $F'' = 0$ can lead to a multiplicity of the solution. This is visible in Fig. 6, where an infinite number of projections is possible from a point O_1 with the coordinate $\zeta = R$ onto an arc BC, and from a point O_2 with the coordinate $\zeta = -R$ onto another arc CD.

4.1.1. Violation of C^2-continuity

The violation of C^2-continuity, but keeping C^1-continuity leads to a discontinuous projection domain. In this case, however, it is easily possible to construct a continuous projection domain, from where uniqueness of the projection operation is automatically fulfilled. The idea is presented in Table 1 and is illustrated in Fig. 6. Since discontinuity is resulting due to the only piecewise continuous parameter ζ, a continuous projection domain is constructed by taking the minimal parameter $\zeta = \min\{R, \infty\} = R$ along the curve.

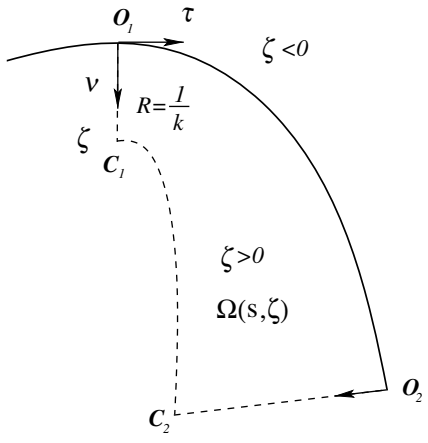

Fig. 5. 2D case – plane curve. Projection domain.

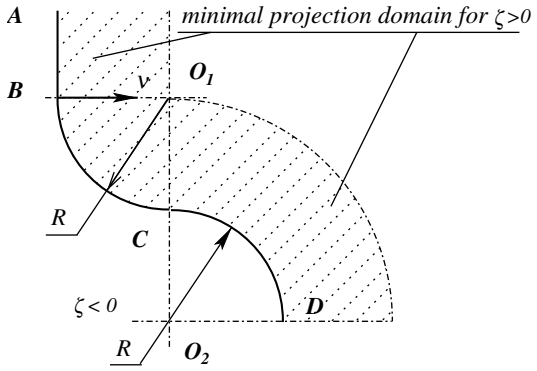

Fig. 6. Violation of C^2-continuity results in changing the discontinuity of the projection domain. A continuous domain is constructed by setting ζ to a minimal value.

Table 1
Violation of C^2-continuity of a curve leads to piecewise continuous curvature and consequently to a piecewise continuous parameter ζ

Part of a curve	Curvature k	Computed ζ	Minimal ζ
A B	0	$+\infty$	R
B C	R	R	R
C D	-R	$+\infty$	R

A continuous projection domain $\Omega(s,\zeta) := \{\mathbf{r} = \boldsymbol{\rho}(s) + \zeta \boldsymbol{v}\}$ can be constructed by setting ζ to a minimal value. An example is given for $\zeta > 0$ in Fig. 6.

4.1.2. Violation of C^1-continuity

We consider here the most practical case which is standard in the triangulation of surfaces with low order finite elements: piecewise differentiable functions with finite jumps for the first derivative. From a geometrical point of view this situation leads to an angular point for curves or an edge for surfaces. The violation of C^1-continuity for a surface parameterization leads also to a discontinuity of the normal vector **n** causing either difficulty with definition of the local coordinate system, or multiplicity of projection. The situation in 2D is presented in Fig. 7. Now, we consider a point following the path $S_1S_2S_3S_4S_5$ in the local coordinate system (28). Since a normal vector $\boldsymbol{v}$ has jumps (points B and C), there are portions of the trajectory which can not be described in this local coordinate system. They are located in the non-allowable domain with regard to the projection onto the curve: any point S_2 laying in the non-allowable domain can not be described in the local coordinate system given by Eq. (28). The term *nonallowable domain with regard to the projection onto surface resp. curve resp. point* is then used for a domain where any point can not be described in the local coordinate system corresponding to the projection onto surface resp. curve resp. point.

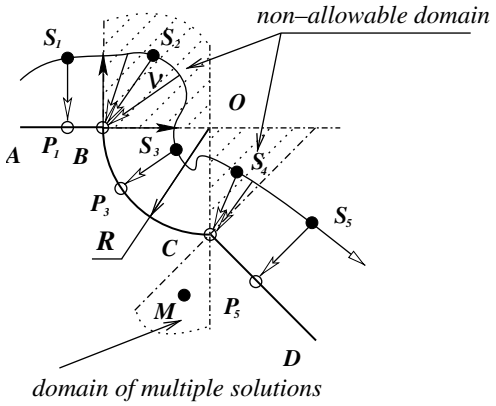

Fig. 7. Violation of C^1-continuity leads to non-allowable domains with regard to the projection onto curve $ABCD$. A special treatment is necessary to preserve a continuous mapping.

However, in such a situation it is possible to create a continuous mapping of the path $S_1S_2S_3S_4S_5$ onto the curve by introducing a new projection operation in the non-allowable domain with regard to the projection onto the curve. This is a projection of the point into an angular point of curves (e.g. S_2 into B and S_4 into C in Fig. 7), or a closest point projection onto the edge of surfaces. This method is mentioned for 2D examples in Heegaard and Curnier [6] and in Zhong and Nilsson [32]; it is also reported to be done, e.g. in LS-DYNA [10]. A projection procedure keeping a continuous mapping of any path on the curve will be called *the generalized closest point procedure*. In 2D cases this procedure includes both a projection onto the curve and onto the corner point.

Another situation arising from the violation of C^1-continuity is overlapping of two or more projection domains causing consequently the multiplicity of projection, see e.g. domain of multiple solutions in Fig. 7.

We already could observe the multiplicity of solutions in the case of the violation of C^2-continuity where the second derivative of the distance function is zero $F'' = 0$, see point O_1 in Fig. 6. In this case, a strong inequality in the formulation of the projection domains allows to eliminate the multiplicity. A case with violation of C^1-continuity (e.g. domain of multiple solutions in Fig. 7) can lead to a more severe situation, see point M passing over corner point C. A natural remedy in this case is to define a minimum distance in the sense of the generalized closest point procedure onto neighboring segments and onto corner point C. However, one can find a line with points which are equidistantly situated from both segments.

In this situation, though relatively seldom in numerical computations due to round-off errors, a choice either with a random selection of projection sides, or with an averaged normal from all projection sides can be applied, implicitly assuming that the distance is fairly small. Within a contact algorithm the storage of the "slave" point path as history variable would be then necessary.

4.2. Proximity domain for globally C^0-continuous surface in 3D

It is necessary to define additional projection procedures in order to create a proximity domain for the 3D space allowing a continuous mapping of any path laying inside,

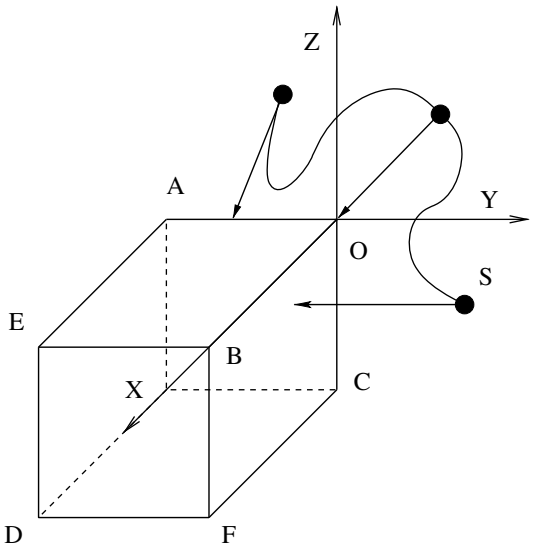

Fig. 8. Hexaedral contact surface in the vicinity of O. A continuous proximity domain (i.e. allowing continuous projection onto the C^1-surface) consist of domains for sides, edges OA, OB, OC and, finally, of a domain for the corner point O.

similar to that discussed for the 2D case in 4.1.2. These projections include a projection onto an edge and onto a corner. The combination of proximity domains leads finally to a continuous domain. The idea is illustrated in Fig. 8 for the contact surface of a hexaeder focusing on the surfaces containing the corner point O. The continuous proximity domain surrounding corner point O consists of

(1) three domains for sides arising from the standard projection procedure:

$S_1 = \{x, y, z \mid x > 0, y > 0, z < 0\}$ for side $BOCF$,
$S_2 = \{x, y, z \mid x > 0, y < 0, z > 0\}$ for side $AOBE$,
$S_3 = \{x, y, z \mid x < 0, y < 0, z < 0\}$ for side AOC;

(2) three domains for edges arising from the point-to-edge projection procedure:

$E_1 = \{x, y, z \mid x < 0, y < 0, z > 0\}$ for edge OA,
$E_2 = \{x, y, z \mid x > 0, y > 0, z > 0\}$ for edge OB,
$E_3 = \{x, y, z \mid x < 0, y > 0, z < 0\}$ for edge OC;

(3) one domain arising from the point-to-corner point projection procedure:

$P = \{x, y, z \mid x < 0, y > 0, z > 0\}$ for corner point O.

The last domain is added to fulfill the continuity, because from this domain a projection onto the cube in general is possible only into a corner point. This projection is trivial, always exists and can be defined simply as difference between "slave" and corner point: $\mathbf{r}_s - \boldsymbol{\rho}_O$.

The point-to-edge projection, in case of a curved edge, requires a numerical solution and again the problem of existence and uniqueness arises.

4.3. Point-to-edge closest point projection and corresponding projection domain

An arbitrary curved edge as a result of the intersection of two surfaces is represented by a curved line, see e.g. AOB in Fig. 9. This line can be parameterized by the arc-length parameter s as well as by an arbitrary parameter ξ, e.g. a normalized coordinate in a finite element approximation:

$$\boldsymbol{\rho} = \boldsymbol{\rho}(s) = \boldsymbol{\rho}(s(\xi)). \tag{34}$$

The transformation of the parameters $s \leftarrow \xi$ is provided by the formula:

$$\mathrm{d}s = \sqrt{\frac{\partial \boldsymbol{\rho}}{\partial \xi} \cdot \frac{\partial \boldsymbol{\rho}}{\partial \xi}}\,\mathrm{d}\xi = \sqrt{\boldsymbol{\rho}_\xi \cdot \boldsymbol{\rho}_\xi}\,\mathrm{d}\xi. \tag{35}$$

The projection routine, though it is looking similar to Eq. (27), is now formulated in 3D as follows:

$$F(s(\xi)) = \frac{1}{2}\left\|\mathbf{r}_s - \boldsymbol{\rho}(s(\xi))\right\|^2 \to \min. \tag{36}$$

The necessary optimum condition leads to the projection operation onto the curve

$$F' = -(\mathbf{r}_s - \boldsymbol{\rho}(s(\xi)) \cdot \frac{\partial \boldsymbol{\rho}}{\partial s} = -(\mathbf{r}_s - \boldsymbol{\rho}(s(\xi)) \cdot \boldsymbol{\tau} = 0, \tag{37}$$

showing the orthogonality of the vector $(\mathbf{r}_s - \boldsymbol{\rho})$ and the tangent vector $\boldsymbol{\tau}$. According to this, a new coordinate system $\boldsymbol{\tau}, \boldsymbol{\nu}, \boldsymbol{\beta}$ is introduced as a natural coordinate system of the curved line, see Fig. 9, where $\boldsymbol{\tau}$ is a unit tangent vector, $\boldsymbol{\nu}$ is a unit main normal vector and $\boldsymbol{\beta}$ is a unit binormal vector of the curve, see [18]. This results in orthogonal planes I, II, III. The given point S ("slave" point) is defined as follows:

$$\mathbf{r}_s = \boldsymbol{\rho}(s) + r\mathbf{e}, \tag{38}$$

where r is the shortest distance between the point S and the curve AB. $\mathbf{e}$ is a vector giving a director of the shortest dis-

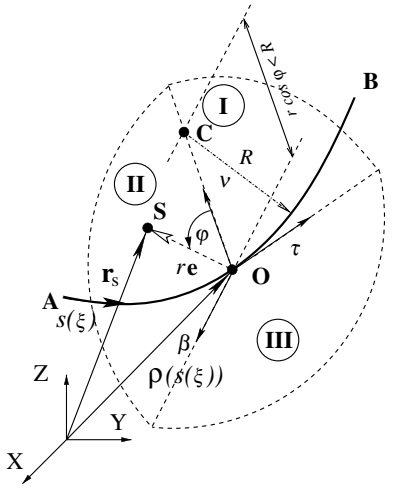

Fig. 9. Point-to-edge projection. Proximity criteria and projection domain.

tance in the plane $\boldsymbol{v0\beta}$ (plane II), defined via $\boldsymbol{v}$ and $\boldsymbol{\beta}$ as follows:

$$\mathbf{e} = \boldsymbol{v}\cos\varphi + \boldsymbol{\beta}\sin\varphi. \tag{39}$$

The second derivative F'' taking into account Eq. (38) is transformed in the curvilinear coordinate system as follows:

$$F'' = \boldsymbol{\tau}\cdot\boldsymbol{\tau} - (\mathbf{r} - \boldsymbol{\rho}(s))\cdot k\boldsymbol{v} = 1 - kr(\mathbf{e}\cdot\boldsymbol{v}) \tag{40}$$

and finally using representation (39) for the vector $\mathbf{e}$ as

$$F'' = 1 - kr\cos\varphi. \tag{41}$$

Considering now $F'' > 0$, the projection domain is constructed from two parts 1 and 2, see Fig. 9:

(1) a semi-infinite domain with negative $\boldsymbol{v}$, or with $\varphi \in [\pi/2, 3\pi/2]$. Here the projection of the vector $r\mathbf{e}$ onto the normal $\boldsymbol{v}$ is negative leading to the automatic satisfaction of $F'' > 0$, and,
(2) a layer with positive $\boldsymbol{v}$, or with $\varphi \in (-\pi/2, \pi/2)$. Here the projection of the vector $r\mathbf{e}$ on the normal $\boldsymbol{v}$ must be less than the radius of the curvature R, i.e.

$$r\cos\varphi < \frac{1}{k} = R. \tag{42}$$

As one can see, two domains surround a curve densely, e.g. without any void. A problem can occur if vector $\boldsymbol{\rho}(s)$ looses C^1-continuity, however in this case we obtain a corner point as discussed above.

Remark 1. If the edge is a straight line then the coordinate system $\boldsymbol{\tau}, \boldsymbol{v}, \boldsymbol{\beta}$ should not be derived via the curved properties of the line according to the Serret–Frenet formulae, however, it can be defined arbitrarily.

In the case of an arbitrary parameterization of a line, the projection routine is fulfilled via the Newton iterative process in Eq. (4) for the parameter ξ, where $\Delta\xi$ is computed as

$$\Delta\xi = -\frac{F'}{F''} = -\frac{(\mathbf{r}_s - \boldsymbol{\rho})\cdot\boldsymbol{\rho}_\xi}{(\boldsymbol{\rho}_\xi\cdot\boldsymbol{\rho}_\xi) - (\mathbf{r}_s - \boldsymbol{\rho})\cdot\boldsymbol{\rho}_{\xi\xi}}, \quad \xi_{(n+1)} = \xi_{(n)} + \Delta\xi. \tag{43}$$

Summary: A continuous projection domain for a globally C^0-continuous surface allowing unique continuous projections of any path laying inside this domain can be constructed via *a generalized projection procedure* including three projection operations: a) onto a surface; b) onto an edge; c) onto a corner point.

Remark 2. An algorithm for the continuous projection domain can be used also as a preparation stage for the global searching routine. Thus, in following computations within an analysis of a contact problem any possible "slave" point can be uniquely projected onto the "master" surface via the corresponding projection onto a surface, an edge or a point.

5. Numerical examples

In this section, we give first a reference example for the construction of the projection domain for a hyperbolical surface, and then discuss a situation where the generalized projection procedure including both, projection onto a segment and onto an edge is needed.

5.1. Reference example: projection domain for a hyperbolical surface

Consider a quadratic surface of the form: $z = (x^2 - y^2)/2$, $0 \leqslant x, y \leqslant 1$ see Fig. 10. The upper projection domain is then a domain between the original surface $OABC$ and the surface $O'A'B'C'$ created by shifting in normal direction as follows:

$$\mathbf{r} = \boldsymbol{\rho}(x,y) + R(x,y)\mathbf{n}(x,y), \quad \boldsymbol{\rho}(x,y) = \{x, y, (x^2 - y^2)/2\}^{\mathrm{T}}, \tag{44}$$

where $R(x,y)$ is a function of the corresponding radius of curvature. Exemplarily, the position of point $C\prime$ is computed as follows. A point on the surface C is defined by the vector $\boldsymbol{\rho} = \{1.000, 0.000, 0.500\}^{\mathrm{T}}$, with the corresponding normal vector $\mathbf{n} = \{-0.707, 0.000, 0.707\}^{\mathrm{T}}$. The main curvatures at point C are computed via Eqs. (16)–(18): $k_1 = 0.354$, $k_2 = -0.700$. A positive value here defines a curvature of a corresponding line which is locally convex with respect to the chosen direction of the normal $\mathbf{n}$, i.e.

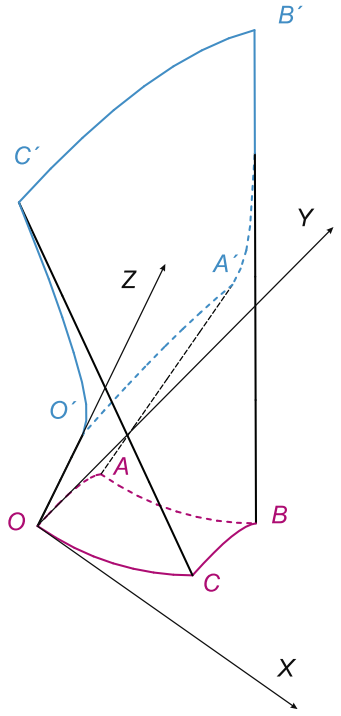

Fig. 10. Structure of the upper proximity domain for a given surface $OABC$ with $z = (x^2 - y^2)/2$, $0 \leqslant x, y \leqslant 1$.

a normal is pointing into a center of curvature of the line. According to the rule for a hyperbolic point discussed in Section 3.2, the value k_1 is taken for the shift as $R_1 = 1/k_1 = 2.825$. Thus, the upper boundary of the projection domain at point C' is computed as $\mathbf{r} = \boldsymbol{\rho} + R_1\mathbf{n} = \{-0.997, 0.000, 2.497\}^{\mathrm{T}}$.

Remark. It is obvious, that the complete algorithm for the projection for an arbitrarily composed CAD surface requires the application of some Boolean operations with domains known from CAD applications. Thus, in general, a fairly large number of cases has to be analyzed within a contact search routine taking advantage of the derived proximity domains.

5.2. Sliding block

This example is intentionally chosen as simple as possible in order to discuss the influence of various contact algorithms on kinematical effects only. A heavy rigid block $ABCD$ with mass m, see Fig. 11 starts to slide (position I) without friction on an inclined surface OE till it is impacting an edge 0 in position II. Assuming frictional contact at the horizontal surface OF, we seek two parameters: the hight H and the friction coefficient μ such that after the impact the block would turn over the edge O in position III without jumping on it until the second impact with a surface OF in position IV. The simplicity of the case allows us to obtain an analytical solution, which we will try to represent numerically. The equation of motion immediately after impacting the edge O (contact only at edge):

$$m\mathbf{a} = \mathbf{R} + m\mathbf{g} \tag{45}$$

leads to the result that a coefficient of friction $\mu > \tan\alpha$ would prevent the block from sliding on the surface OF. An equation for the angular momentum is involved in a polar coordinate system in order to get the information about the possibility of jumping. The full set of equations is then written as

$$\begin{aligned} J_O\ddot{\varphi} &= mga\frac{\sqrt{2}}{2}\sin\varphi \\ ma\frac{\sqrt{2}}{2}\ddot{\varphi} &= mg\sin\varphi + R_\tau \\ ma\frac{\sqrt{2}}{2}\dot{\varphi}^2 &= mg\cos\varphi + R_\nu, \end{aligned} \tag{46}$$

where a is an edge of the cube, J_O is the moment of inertia about the edge O. The solution leads to the reaction force $R_\nu = 5mg\cos\varphi/2 - 3mg/2 - ma\sqrt{2}/2\dot{\varphi}_0^2$. Defining via the energy theorem the initial angular velocity $\dot{\varphi}_0$ after the impact, we finally obtain $R_\nu = 5mg\cos\varphi/2 - mgL\sqrt{2}/a - 3mg/2$. If the reaction is positive $R_\nu > 0$, the block will not jump before the second contact along the side CD occurs (i.e. $\cos\varphi = 45^\circ$). The sliding length L satisfies the following inequality:

$$L < a\left(5\sqrt{2} - 6\right). \tag{47}$$

Now, we model this problem via the node-to-segment approach (NTS), see the FE algorithms in [30,19]. The full problem is modeled with only three finite elements, see Fig. 11b. A penalty approach to enforce contact conditions is applied and a Newmark time integration scheme is used. Inclined and horizontal segments are chosen to be "master" segments, then nodes from the cube are "slaves". It is obvious to see, that during the rotation of the block over the edge the slave nodes are running through a non-allowable domain for the segment projection procedure. This leads to the impossibility to describe the rotation. This artefact causes the block to jump on the second segment, see screen-shots in Fig. 12.

Several possibilities to get a correct solution exist, e.g. Heege and Alart [8] mentioned that correct forces can be recovered as a superposition of forces from neighboring segments within a full Lagrange multiplier method. Another of the possible remedies (also reported in [10])

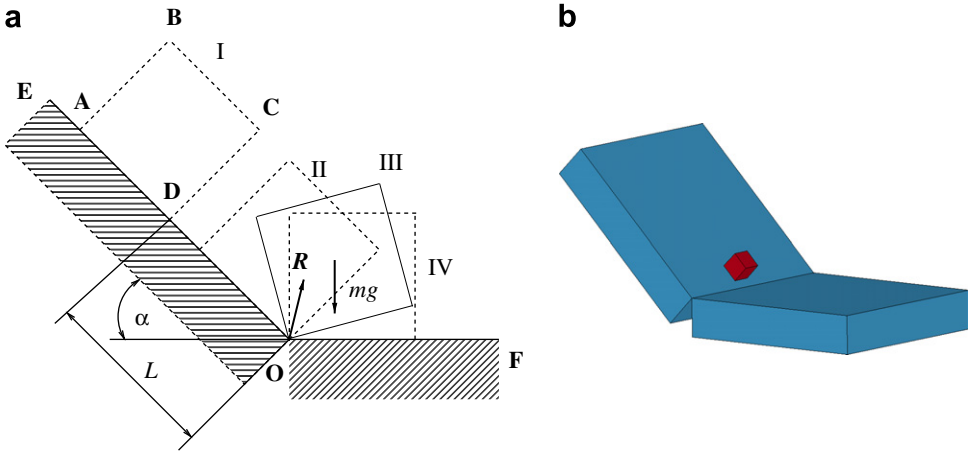

Fig. 11. a) Process of sliding cube b) and its finite element model.

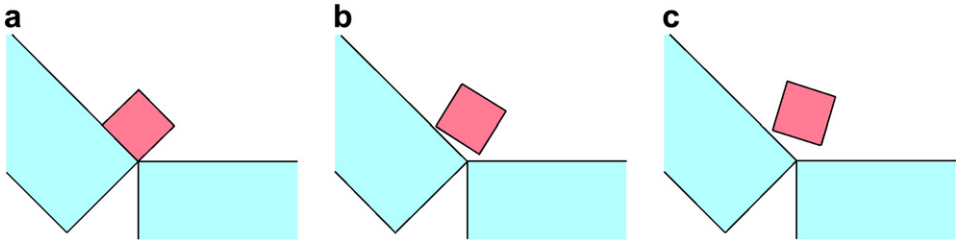

Fig. 12. Absence of the projection of the slave node onto the edge in the contact algorithm (only Node-to-Segment approach) leads to the impossibility to capture the rotational part of the motion. (a) cube impacting the edge, (b) and (c) results of artefact: block jumps on the second segment.

to recover a correct force as a superposition is to allow an overlapping of segments and, therefore, double projections on both segments at the same time. However, this does not solve the problem completely and also leads to jumping. Thus, an additional projection onto the edge needs to be included into the contact algorithm within a penalty approach. But since, the penalty parameter plays the role of an additional spring hanging on the edge, this in general leads to unnecessary vibrations. Then only a careful selection of the penalty parameters leads to acceptable results leading to a rotational motion. This shows that correct kinematics are hard to achieve within a penalty approach. A full Lagrange multiplier method together with a generalized projection procedure would cover the kinematics of this specific example more exactly, allowing, e.g. sliding along the edge.

Remark. The finite element model described above requires also additional contact elements such as a node-to-edge element. The simple version with a linear edge has been implemented so-far for the current example, see also Wriggers [30]. For the fully nonlinear element for curvilinear edges also the application the covariant approach for kinematics as well as for linearization is needed, which is out of scope of the current contribution.

6. Conclusion

In this contribution fundamental problems of existence and uniqueness of the closest point projection procedure are investigated. The analysis is given in a surface coordinate system, which has also been a basis for a covariant description of the contact. The consideration of the differential properties of smooth surfaces allows to create "projection domains" from which a projection of, e.g. a slave node is uniquely defined. For arbitrary C^0 continuous surfaces a projection routine should be generalized to include projections not only onto surfaces, but also onto objects of lower geometrical dimension, such as curved lines and points. The corresponding criteria of existence and uniqueness and, therefore, projection domains are also given in the contribution. The general results are illustrated within a simple example, where the lack of a fully generalized projection scheme may result in a completely different kinematical behavior.

References

[1] ABAQUS, Theory Manual, 2007. <http://www.abaqus.com/>.
[2] P. Alart, A. Curnier, A mixed formulation for frictional contact problems prone to Newton like solution methods, Comput. Methods Appl. Mech. Engrg. 92 (1991) 353–375.
[3] D.P. Bertsekas, Convex Analysis and Optimization, Athena Scientific, Belmont, Mass, 2003.
[4] A.E. Giannakopoulos, The return-mapping method for the integration of friction constitutive relations, Comput. Struct. 32 (1) (1989) 157–167.
[5] J.Q. Hallquist, G.L. Goudreau, D.J. Benson, Sliding interface with contact-impact in large-scale Lagrangian computations, Comput. Methods Appl. Mech. Engrg. 51 (1985) 107–137.
[6] J.-H. Heegaard, A. Curnier, An augmented Lagrangian method for discrete large-slip contact problems, Int. J. Numer. Methods Engrg. 36 (1993) 569–593.
[7] J.-H. Heegaard, A. Curnier, Geometric properties of 2D and 3D unilateral large slip contact operators, Comput. Methods Appl. Mech. Engrg. 131 (1996) 263–286.
[8] A. Heege, P. Alart, A frictional contact element for strongly curved contact problems, Int. J. Numer. Methods Engrg. 39 (1996) 165–184.
[9] S. Hüeber, B.I. Wohlmuth, Large deformation frictional contact mechanics: continuum formulation and augmented Lagrangian treatment, Comput. Methods Appl. Mech. Engrg. 194 (2005) 3147–3166.
[10] LS-DYNA, Theoretical Manual, Livermore Software Technology Corporation (compiled by Hallquist J.O.), 2007. <http://www.lstc.com/>.
[11] R.E. Jones, P. Papadopoulos, A yield-limited Lagrange multiplier formulation for frictional contact, Int. J. Numer. Methods Engrg. 48 (2000) 1127–1149.
[12] N. Kikuchi, J.T. Oden, Contact Problems in Elasticity: A Study of Variational Inequalities and Finite Element Methods, SIAM, Philadelphia, 1988.
[13] A. Konyukhov, K. Schweizerhof, Contact formulation via a velocity description allowing efficiency improvements in frictionless contact analysis, Comput. Mech. 33 (2004) 165–173.
[14] A. Konyukhov, K. Schweizerhof, Covariant description for frictional contact problems, Comput. Mech. 35 (2005) 190–213.
[15] A. Konyukhov, K. Schweizerhof, A special focus on 2D formulations for contact problems using a covariant description, Int. J. Numer. Methods Engrg. 66 (2006) 1432–1465.
[16] A. Konyukhov, K. Schweizerhof, Covariant description of contact interfaces considering anisotropy for adhesion and friction, Part 1, Comput. Methods Appl. Mech. Engrg. 196 (1–3) (2006) 103–117.
[17] A. Konyukhov, K. Schweizerhof, Covariant description of contact interfaces considering anisotropy for adhesion and friction, Part 2, Comput. Methods Appl. Mech. Engrg. 196 (1–3) (2006) 289–303.
[18] S. Lang, Fundamentals of Differential Geometry, Springer, New York, Heidelberg, 2001.
[19] T.A. Laursen, Computational Contact and Impact Mechanics. Fundamentals of Modeling Interfacial Phenomena in Nonlinear Finite Element Analysis, Springer, 2002.

[20] T.A. Laursen, J.C. Simo, A continuum-based finite element formulation for the implicit solution of multibody large deformation frictional contact problems, Int. J. Numer. Methods Engrg. 35 (1993) 3451–3485.
[21] H. Parisch, A consistent tangent stiffness matrix for three-dimensional nonlinear contact analysis, Int. J. Numer. Methods Engrg. 28 (1989) 1803–1812.
[22] H. Parisch, Ch. Lübbing, A formulation of arbitrarily shaped surface elements for three-dimensional large deformation contact with friction, Int. J. Numer. Methods Engrg. 40 (1997) 3359–3383.
[23] D. Peric, D.R.J. Owen, Computational model for 3D contact problems with friction based on the penalty method, Int. J. Numer. Methods Engrg. 35 (1992) 1289–1309.
[24] G. Pietrzak, A. Curnier, Large deformation frictional contact mechanics: continuum formulation and augmented Lagrangian treatment, Comput. Methods Appl. Mech. Engrg. 177 (1999) 351–381.
[25] M.A. Puso, T.A. Laursen, A mortar segment-to-segment contact method for large deformation solid mechanics, Comput. Methods Appl. Mech. Engrg. 193 (2004) 601–629.
[26] M.A. Puso, T.A. Laursen, A mortar segment-to-segment frictional contact method for large deformations, Comput. Methods Appl. Mech. Engrg. 193 (2004) 4891–4913.
[27] J.C. Simo, T.J.R. Hughes, Elastoplasticity and Viscoplasticity: Computational Aspects, Springer, Berlin, 1992.
[28] P. Wriggers, J.C. Simo, A note on tangent stiffness for fully nonlinear contact problems, Commun. Appl. Numer. Methods 1 (1985) 199–203.
[29] P. Wriggers, Van Vu, E. Stein, Finite element formulation of large deformation impact–contact problems with friction, Comput. Struct. 37 (1990) 319–331.
[30] P. Wriggers, Computational Contact Mechanics, second ed., Springer, 2006.
[31] Z.-H. Zhong, Finite Element Procedures for Contact–Impact Problems, Oxford University Press, Oxford, 1993.
[32] Z.-H. Zhong, L. Nilsson, A unified contact algorithm based on the territory concept, Comput. Methods Appl. Mech. Engrg. 130 (1996) 1–16.